Journal of Thermal Science Vol.31, No.2 (2022) 436–447

https://doi.org/10.1007/s11630-022-1583-z **Article ID: 1003-2169(2022)02-0436-12**

Flexible Operation Mode of Coal-fired Power Unit Coupling with Heat Storage of Extracted Reheat Steam

WEI Haijiao[1], LU Yuanwei[1*], YANG Yanchun[1], ZHANG Cancan[1], WU Yuting[1], LI Weidong[2], ZHAO Dongming[2]

1. MOE Key Laboratory of Enhanced Heat Transfer and Energy Conservation, Beijing Key Laboratory of Heat Transfer and Energy Conversion, Faculty of Environment and Life, Beijing University of Technology, Beijing 100124, China
2. China Huaneng Group Clean Energy Research Institute Co. Ltd, Beijing 102209, China

Abstract: In order to provide more grid space for the renewable energy power, the traditional coal-fired power unit should be operated flexibility, especially achieved the deep peak shaving capacity. In this paper, a new scheme using the reheat steam extraction is proposed to further reduce the load far below 50% rated power. Two flexible operation modes of increasing power output mode and reducing fuel mode are proposed in heat discharging process. A 600 MW coal-fired power unit with 50% rated power is chosen as the research model. The results show that the power output is decreased from 300.03 MW to 210.07 MW when the extracted reheat steam flow rate is 270.70 $t \cdot h^{-1}$, which increases the deep peak shaving capacity by 15% rated power. The deep peak shaving time and the thermal efficiency are 7.63 $h \cdot d^{-1}$ and 36.91% respectively for the increasing power output mode, and they are 7.24 $h \cdot d^{-1}$ and 36.58% respectively for the reducing fuel mode. The increasing power output mode has the advantages of higher deep peak shaving time and the thermal efficiency, which is recommended as the preferred scheme for the flexible operation of the coal-fired power unit.

Keywords: coal-fired power unit, flexible operation, deep peak shaving, extracted reheat steam, heat storage

1. Introduction

Increasing the proportion of renewable energy power and reducing the thermal power can reduce the carbon emissions significantly [1, 2]. China aims to achieve carbon peak in 2030 and carbon neutralization in 2060 [3], which means that developing renewable energy is China's future national policy. At the end of 2020, the total installed capacity of electric power in China has reached 2200.58 GW, of which the installed capacity of renewable energy accounts for 42.4%. And the total electric power generation of China was 7 147 000 GWh in 2020, of which the electricity generated by renewable energy only accounted for 7.51%. The data shows that although the installed capacity of renewable energy accounts for a large proportion, the proportion of renewable energy power generation into the grid is lower due to its intermittence and instability. How to improve this situation is an urgent problem to be solved. Therefore, the power generation from the traditional coal-fired power unit (CFPU) should be reduced to allow large-scale renewable energy power generation into the fixed capacity grid [2, 4]. In the future, the traditional CFPU will need to be altered from the main power

Received: Sep 26, 2021 AE: LIU Zhijian Corresponding author: LU Yuanwei E-mail: luyuanwei@bjut.edu.cn

Nomenclature

Symbols

B	coal consumption rate/g·kW^{-1}·h^{-1}
c_p	specific heat of molten salt at constant pressure/J·kg^{-1}·K^{-1}
G	mass flow rate/t·h^{-1}
h	specific enthalpy/kJ·kg^{-1}
LHV	lower heating value of coal/kJ·kg^{-1}
p	pressure/kPa
Q	heat power/MW
q	enthalpy difference of steam/kJ·kg^{-1}
T	thermodynamic temperature/K
W	power output of the unit/MW

Abbreviations

CFPU	coal-fired power unit
CP	condensate water pump
CT	cold molten salt tank
FP	feed water pump
HPT	high pressure steam turbine
HT	hot molten salt tank
IPT	intermediate pressure steam turbine
IPM	increasing power output mode
LPT	low pressure steam turbine
MWHE	molten salt-water heat exchanger
PWT	pressurized water tank
RH	regenerative heat exchanger
RFM	reducing fuel mode
SWHE	steam-water heat exchanger
SMHE	steam-molten salt heat exchanger
TV	throttle valve
WT	water tank

Greek symbols

τ	Time/h
γ	enthalpy difference of drainage water/kJ·kg^{-1}
φ	enthalpy difference of water/kJ·kg^{-1}

Subscripts

c	exhaust steam of low pressure steam turbine
cha	heat charging process
coal	coal into the boiler
cond	condensate water
cond,by	bypassed condensate water
c-salt	low temperature molten salt
dw	drainage water
discha	heat discharging process
feed	feed water
feed,by	bypassed feed water
h-salt	high temperature molten salt
ms	molten salts
pw	pressurized water
r	reheat steam
s	main steam
sd	drainage water of extracted steam
sT	stage of turbine
T	turbine
w	water
0	parameters before off-design

generation mode to the flexible operation mode [2, 5], so it is important to investigate the flexible operation mode of coal-fired power unit to let more renewable power generation access to the power grid.

In the past, for the renewable energy installed capacity was small, the renewable energy power generation has less impact on the grid, so the main role of CFPU is to increase the ramp rate of the unit under the off-design conditions [6, 7] to satisfy the requirements of renewable energy power access to the grid. Wang et al. [8] found that a revised water fuel ratio control strategy could raise the flexible operation of supercritical CFPU by increasing the ramp rate from 10 MW·min^{-1} to 30 MW·min^{-1} under the load from 50% to 100%. Zhang et al. [9] adopted the condensate throttling method to fast change the unit load by 4.04% under the 100% rated load. Wang et al. [10] revised the bypassed feed water mode, and the dynamic response rate increased two times under the load from 40% to 100%. Zhao et al. [11] analyzed the influence of steam extraction throttling methods of the regenerative heater on the ramp rate of the unit, and found that the maximum average power ramp rate in a minute is 6.19% rate power by adopting the throttling method of 1st–3rd regenerative heater under the load from 50% to 100%, which greatly improved the flexible operation of the unit. Wang et al. [12] regulated the coordinated control strategy and the heat source regulation mode to increase the ramp rate of the unit to 13.20 MW·min^{-1} under the 87.12% rated load, with the help of the characteristics of large thermal inertia of district heating network. The above researches show that improving the ramp rate of the unit can increase the load changing ability of the unit instantaneously. So that the small-scale fluctuating renewable energy can be smoothly accessed to the grid. However, with the future increasing installed capacity of renewable energy, the limited regulating capacity of this method cannot provide enough space for large-scale renewable energy power generation.

In order to provide enough space for renewable energy power generation access to the grid, the flexible operation of the unit was proposed [13, 14]. From the perspective of power generation side, broadening the operation range of the unit under stable load is the most effective means to realize the flexible operation. Richter et al. [15] studied that the unit load could be reduced to 93% from 100% through hot water storage without changing the operation mode of CFPU. Trojan et al. [16] investigated that integrated hot water storage into CFPU could reduce the unit load from 76.50% to 56.52%. Li et al. [17] reduced the load of 600 MW unit from 100% rated load to 86.70% rated load by using the reheat steam extraction and heat storage. Krüger et al. [18] integrated the thermal energy storage into the steam power plants to regulate the load range, and found that the output power was decreased by 4% under 100% rated load in heat charging process. Those studies proved that the utilization of the steam extraction can achieve the flexible operation of the CFPU under the stable load. However, the previous studies are mostly focused on the load regulation from 100% rate power by extracted steam and heat storage. With the increasing demand for flexible operation of CFPU, the deep peak shaving capacity under lower load operation should be proposed.

Generally, the unit load reduction capacity is limited by the minimum stable combustion load of 40% rated power [19, 20] and the minimum denitration parameters of 45% rated power [20]. This research studied the load regulation in different operation modes during flexible operation of CFPU; the flexible operation scheme takes the stable unit load of 50% rated power as the peak shaving base load. Wei et al. [21] studied on the flexible operation of coal-fired power unit by main steam extraction to further reduce the load from the 50% rated load. For the higher exergy loss of the main steam extraction flow through a throttle valve, a new scheme using the reheat steam extraction is proposed to further reduce the load of CFPU far below 50% rated load. The sensible heat and latent heat of the extracted reheat steam are stored in molten salt and pressurized water, respectively, during the heat charging process. The stored heat in molten salts is returned to heat the bypassed feed water and the stored pressurized water replaces the condensate water in the heat discharging process. The proposed system can provide two heat discharging modes: increasing power output mode (IPM) and reducing fuel mode (RFM). Such a scheme has not been found in the published journals. The innovation of this paper is that on the one hand, the load reduction operation is conducted at 50% rate load of the unit to be further reduced by 15%; on the other hand, two heat discharging models are constructed to achieve the flexible operation of CFPU. The objectives of this paper is to investigate the relationship between the extracted reheat steam flow rate and the deep load reduction capacity, and analyze the thermal performance of CFPU by IPM and RFM separately to complete the deep peak shaving. The deep peak shaving time and the influence of the pressure of pressurized water on IPM and RFM were studied.

2. Flexible Operation System of CFPU by Heat Storage

2.1 Flexible operation system

A 600 MW subcritical CFPU was chosen as a research model. The flexible operation system includes the traditional coal-fired power unit, the heat charging and discharging systems, as shown in Fig. 1 and Fig. 2.

The workflow of the traditional CFPU is described as follows. The main steam from the boiler enters the high pressure steam turbine (HPT) for expansion. The exhaust steam of HPT enters the boiler for reheating and then enters the intermediate pressure steam turbine (IPT) and low pressure steam turbine (LPT) successively. The exhaust steam of LPT enters the condenser to condense it into saturated water. The condensate water (low pressured water) is successively pumped into the 7th regenerative heater (RH7), RH6 and RH5 by the condensate pump (CP), and then enters the RH4. The feed water (high pressured water) in RH4 is successively pumped into RH3, RH2 and RH1 by feed pump (FP), and enters the boiler again to generate main steam. The heating steam source of RH1-RH7 is from the steam extraction port of the intermediate stages of the turbine. The drainage water of the previous regenerative heater enters the next stage regenerative heater by the step-by-step flow mode; namely the drainage water of RH1 flows through RH2 and RH3, and enters RH4, and the drainage water of RH5 flows through RH6 and RH7, and finally enters the condenser. In this way, the thermal cycle of the traditional CFPU is completed.

In the traditional CFPU, its rated power of the subcritical CFPU is 600.18 MW. The 50% rated power (300.11 MW) is chosen as the basic operation load for further deep peak shaving, and the parameters of 50% rated power are selected as the basic research parameters. Table 1 shows the designed parameters of each nodes of the subcritical CFPU at 50% rated power.

For the deep peak shaving of CFPU, a part of the reheat steam is extracted and isenthalpic depressurized in the throttle valve (TV), and then enters the steam-molten salt heat exchanger (SMHE) to heat the molten salts that coming from the cold molten salt tank (CT) to the hot molten salt tank (HT). The cooled extracted steam enters into the steam-water heat exchanger (SWHE) to heat the pressurized water from water tank (WT). The pressurized water is stored in pressurized water tank (PWT). The extracted reheat steam condenses in the SWHE and flows back to the condenser.

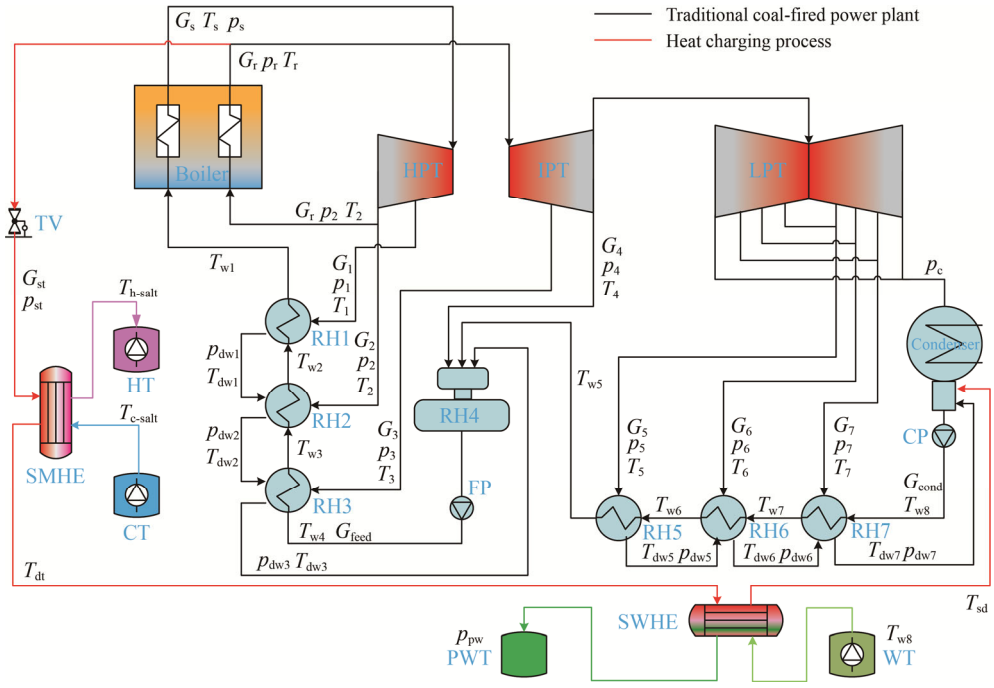

Fig. 1 Heat charging diagram of CFPU

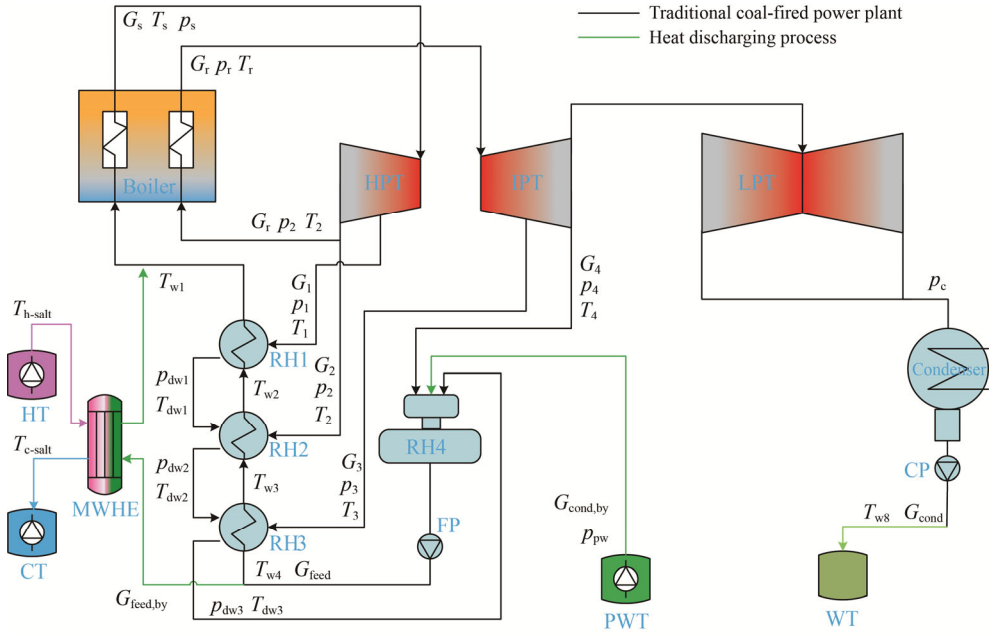

Fig. 2 Heat discharging diagram of CFPU

During the flexible operation process, a kinds of binary mixed nitrate molten salts [22] and pressurized water are selected as the heat storage medium. The molten salts are used to store the sensible heat of the extracted reheat steam in the SMHE during the heat charging process and to heat the bypassed feed water in the heat discharging process. The thermophysical properties of molten salts are shown in Table 2. The pressurized water is chosen for storing the latent heat of the extracted reheat steam due to its higher heat storage density.

The heat discharging process of CFPU is described as follows in Fig. 2. The steam generated by the boiler and the working fluid are same as that of the traditional CFPU. The steam condenses in the condenser and is stored in the WT. The pressurized water in the PWT enters RH4 and replaces all the condensate water of RH5-RH7, so the power output of LPT can be increased. Part of the feed water of RH4 enters RH3, RH2, RH1 and boiler, while the other part of the feed water of RH4 enters the molten salt-water heat exchanger (MWHE) and

Table 1 Designed parameters of the subcritical CFPU at 50% rated power

Node	p/kPa	T/K	G/t·h^{-1}	Node	p/kPa	T/K	G/t·h^{-1}
s	9774	811.15	900.11	w5	1724	425.25	751.97
r	1750	811.15	789.27	w6	1724	375.45	751.97
1	3094	650.95	46.84	w7	1724	346.68	751.97
2	1944	590.75	48.09	w8	1724	327.12	751.97
3	1059	737.25	26.04	dw1	3001	488.15	46.84
4	530	638.45	23.19	dw2	1886	458.85	95.65
5	324	581.35	35.98	dw3	1006	435.15	121.69
6	128	475.65	33.98	dw5	308	381.05	35.98
7	43	370.96	22.15	dw6	121	352.28	69.96
w1	18 227	508.65	900.11	dw7	40.8	333.81	92.10
w2	18 227	482.55	900.11	cp	1724	–	751.97
w3	18 227	453.25	900.11	fp	18 227	–	900.11
w4	18 227	429.55	900.11	c	15	–	659.03

Table 2 Thermophysical parameters of molten salts

Categories	Parameters
Components	KNO_3-$Ca(NO_3)_2$
Temperature range/K	463.15 to 833.15
Density/kg·m^{-3}	2357.57–0.6757T
Specific heat/kJ·kg^{-1}	1.12+6.11×10^{-4}T

is heated by the high temperature molten salts that coming from HT to CT. The heated feed water temperature is same as the outlet temperature of RH1, and the heated feed water enters the boiler, so the steam extraction from HPT and IPT can be decreased and the power output also can be increased. The cooled molten salts flows back to CT. Thus, the thermal discharging cycle is completed.

2.2 Flexible operation mode

It can be seen from Section 2.1 that the stored heat can be released to the CFPU in the peak period of power consumption during the heat discharging process and the power output can be increased because the steam extraction flow rate of RH from the turbine can be decreased, so this heat discharging mode is designed as the IPM. Also, in general, when the power output remains constant (such as 300.03 MW) in the period of fixed power consumption, the coal mass flow rate into the boiler can be reduced during the heat discharging process because the flow rate of stream out of the boiler can be decreased to offset the increase in power output from the decrease in the steam extraction of RH from turbine. This heat discharging mode is defined as the RFM.

The extracted steam pressure (p_{st}) and temperature (T_{st}) behind the throttle valve is 500 kPa and 805.66 K, respectively. The outlet temperatures of SHME (T_{dt}) and SWHE (T_{sd}) are 473.15 K and 332.72 K, and the molten salts temperatures of HT ($T_{h\text{-}salt}$) and CT ($T_{c\text{-}salt}$) are 463.15 K and 633.15 K, respectively. The pressure of the conventional pressurized water storage tank is 200 kPa [23]. In order to understand the pressure influence of the pressurized water on heat charging and heat discharging processes, the pressurized water of 200 kPa and higher pressurized water of 400 kPa are selected as the research parameters. Therefore, according to the heat discharging operation modes and the pressure of the pressurized water, the flexible operation modes in heat discharging process of CFPU can be divided into four operating conditions, as shown in Table 3.

Table 3 Flexible operation modes in heat discharging process of CFPU

Heat discharging process	Heat charging process	Parameters of pressurized water
IPM-I	p_{pw}=200 kPa	p_{pw}=200 kPa, T_{pw}=393.36 K
IPM-II	p_{pw}=400 kPa	p_{pw}=400 kPa, T_{pw}=416.76 K
RFM-I	p_{pw}=200 kPa	p_{pw}=200 kPa, T_{pw}=393.36 K
RFM-II	p_{pw}=400 kPa	p_{pw}=400 kPa, T_{pw}=416.76 K

3. Methodology

The first law of thermodynamics is chosen to investigate the flexible operation of CFPU.

3.1 Heat balance equation of flexible operation of CFPU

According to the equation of flexible operation of CFPU described in Ref. [21], a new heat balance equation of the flexible operation of CFPU by integrated with reheat steam extraction is obtained, which is shown in Eq. (1).

$$\begin{bmatrix} q_1 & & & & & & \\ \gamma_2 & q_2 & & & & & \\ \gamma_3 & \gamma_3 & q_3 & & & & \\ \gamma_4 & \gamma_4 & \gamma_4 & q_4 & & & \\ & & & & q_5 & & \\ & & & & \gamma_6 & q_6 & \\ & & & & \gamma_7 & \gamma_7 & q_7 \end{bmatrix} \begin{bmatrix} G_1 \\ G_2 \\ G_3 \\ G_4 \\ G_5 \\ G_6 \\ G_7 \end{bmatrix} = \begin{bmatrix} (G_{\text{feed}} - G_{\text{feed,by}})\varphi_1 \\ (G_{\text{feed}} - G_{\text{feed,by}})\varphi_2 \\ (G_{\text{feed}} - G_{\text{feed,by}})\varphi_3 \\ (G_{\text{cond}} - G_{\text{cond,by}})\varphi_4 + G_{\text{cond,by}}(h_4 - h_{\text{pw}}) \\ (G_{\text{cond}} - G_{\text{cond,by}})\varphi_5 \\ (G_{\text{cond}} - G_{\text{cond,by}})\varphi_6 \\ (G_{\text{cond}} - G_{\text{cond,by}})\varphi_7 \end{bmatrix} \tag{1}$$

where, q_j, γ_j and φ_j are calculated by Eqs. (2)–(4) [21, 24].

$$q_j = h_j - h_{\text{dw},j} \tag{2}$$

$$\gamma_j = h_{\text{dw},j\text{-}1} - h_{\text{dw},j} \tag{3}$$

$$\varphi_j = h_{\text{w},j} - h_{\text{w},j+1} \tag{4}$$

where, j is the regenerative heater number (j=1,2,⋯,7).

In traditional CFPU and charging process, $G_{\text{feed,by}}$ and $G_{\text{cond,by}}$ are 0. In discharging process, $G_{\text{feed,by}}$ and $G_{\text{cond,by}}$ are variables.

The power output of CFPU can be calculated by Eq. (5) after calculating the Eq. (1).

$$\begin{aligned} W_{\text{T}} = \Big\{ & G_{\text{s}}(h_{\text{s}} - h_1) + (G_{\text{s}} - G_1)(h_1 - h_2) \\ & + (G_{\text{s}} - G_1 - G_2)(h_{\text{r}} - h_3) \\ & + \sum_{m=3}^{6} \left[\left(G_{\text{s}} - \sum_{j=1}^{m} G_{\text{j}} \right)(h_m - h_{m+1}) \right] \\ & + \left(G_{\text{s}} - \sum_{j=1}^{7} G_j \right)(h_7 - h_{\text{c}}) \Big\} \Big/ 3600 \end{aligned} \tag{5}$$

The combustion and heat balance equations is calculated by Eq. (6) [24].

$$G_{\text{coal}} \text{LHV} \eta_{\text{b}} = G_{\text{s}}(h_{\text{s}} - h_{\text{w1}}) + G_{\text{r}}(h_{\text{r}} - h_2) \tag{6}$$

where, LHV is 29 270 kJ·kg^{-1}; η_{b} is the thermal efficiency of the boiler, which is 93.36%.

3.2 Heat balance equation of heat charging and discharging processes

The sensible heat of the extracted reheat steam is stored by using the molten salts, and the sensible heat charging power of the SMHE is calculated by Eq. (7). The latent heat of the extracted reheat steam is stored by using the pressurized water, and the latent heat charging power of the SWHE is calculated by Eq. (8).

$$Q_{\text{cha.SMHE}} = \frac{G_{\text{st}}(h_{\text{r}} - h_{\text{dt}})}{3600} = \frac{G_{\text{cha.ms}} c_p (T_{\text{h-salt}} - T_{\text{c-salt}})}{3600\eta} \tag{7}$$

$$Q_{\text{cha.SWHE}} = \frac{G_{\text{st}}(h_{\text{dt}} - h_{\text{sd}})}{3600} = \frac{G_{\text{pw}}(h_{\text{pw}} - h_{\text{w8}})}{3600\eta} \tag{8}$$

where, η is the thermal efficiency of the heat exchanger, which is 98%.

The total heat charging power of the extracted reheat steam is defined by Eq. (9).

$$Q_{\text{cha}} = Q_{\text{cha.SMHE}} + Q_{\text{cha.SWHE}} \tag{9}$$

The stored sensible heat is released to heat the bypassed feed water, and the heat discharging power of the MWHE is calculated by Eq. (10). The stored pressurized water is pumped to RH4 to replace the condensate water, and its heat discharging power is calculated by Eq. (11).

$$\begin{aligned} Q_{\text{discha.MWHE}} &= \frac{G_{\text{feed,by}}(h_{\text{w1}} - h_{\text{w4}})}{3600} \\ &= \frac{\eta G_{\text{discha.ms}} c_p (T_{\text{h-salt}} - T_{\text{c-salt}})}{3600} \end{aligned} \tag{10}$$

$$Q_{\text{discha.pw}} = \frac{G_{\text{cond,by}}(h_{\text{pw}} - h_{\text{w8}})}{3600} \tag{11}$$

The total heat discharging power is defined by Eq. (12).

$$Q_{\text{discha}} = Q_{\text{discha.MWHE}} + Q_{\text{discha.pw}} \tag{12}$$

In the process of heat charging and heat discharging, the ratio of the sensible heat charging power to the total heat charging power must be equal to the ratio of the sensible heat discharging power to total heat discharging power, as shown in Eq. (13).

$$\frac{Q_{\text{cha.SMHE}}}{Q_{\text{cha}}} = \frac{Q_{\text{discha.MWHE}}}{Q_{\text{discha}}} \tag{13}$$

Due to the off-design condition caused by the extracted reheat steam, the steam flow rate into the stage of the turbine is changed. The off-design model of the stage should be recalculated by Eq. (14) [25].

$$\frac{G_{\text{sT},i}}{G_{\text{sT0},i}} = \sqrt{\frac{p_{\text{sT},i}^2 - p_{\text{sT},i+1}^2}{p_{\text{sT0},i}^2 - p_{\text{sT0},i+1}^2}} \sqrt{\frac{T_{\text{sT},i}}{T_{\text{sT0},i}}} \tag{14}$$

where, i is the number of turbine stages (i=1,2,⋯,8).

3.3 Evaluating indicator of flexible operation system of CFPU

3.3.1 Deep peak shaving time

When the flexible operation of coal-fired power unit completes the process of heat charging and heat discharging, the relationship between charging time and discharging time is the key factor to determine the deep peak shaving time of CFPU. The charging time refers to the load reduction time when the heat of the extracted

reheat steam is stored in the heat storage system. The discharging time means the heat release time when all the stored heat is released to the CFPU. The deep peak shaving time refers to the total time of multiple load reduction every day by steam extraction. The relationship between charging time and discharging time is calculated by the ratio of discharging time to charging time, as shown in Eq. (15). The deep peak shaving time is calculated by Eq. (16).

$$\theta=\frac{\tau_{\text{discha}}}{\tau_{\text{cha}}}=\frac{Q_{\text{cha}}\eta\varepsilon}{Q_{\text{discha}}} \tag{15}$$

$$\tau_{\text{deep}}=\frac{24}{1+\theta} \tag{16}$$

where, θ is the ratio of discharging time to charging time; ε is the coefficient of heat preservation of HT and PWT, which is 95%; τ_{deep} is the deep peak shaving time, $\text{h}\cdot\text{d}^{-1}$.

3.3.2 Thermal efficiency and coal consumption rate

The thermal efficiency and coal consumption rate are two important indicators to evaluate the thermal performance of the CFPU by completing the deep peak shaving. The thermal efficiency of the traditional CFPU is calculated according to Eq. (17), and the thermal efficiency of the CFPU completing the flexible operation is calculated according to Eq. (18).

$$\eta_{\text{thermal}}=\frac{3600W_{\text{T}}}{G_{\text{coal}}\text{LHV}}\times100\% \tag{17}$$

$$\eta_{\text{thermal}}=\frac{3600\left(W_{\text{cha.T}}\tau_{\text{cha}}+W_{\text{discha.T}}\tau_{\text{discha}}\right)}{\left(G_{\text{cha.coal}}\tau_{\text{cha}}+G_{\text{discha.coal}}\tau_{\text{discha}}\right)\text{LHV}}\times100\% \tag{18}$$

where, η_{thermal} is the thermal efficiency, %.

The coal consumption rate of the traditional CFPU is calculated by Eq. (19), and the coal consumption rate of the CFPU completing the flexible operation is calculated by Eq. (20).

$$B=\frac{1000G_{\text{coal}}}{W_{\text{T}}} \tag{19}$$

$$B=\frac{1000\left(G_{\text{cha.coal}}\tau_{\text{cha}}+G_{\text{discha.coal}}\tau_{\text{discha}}\right)}{W_{\text{cha.T}}\tau_{\text{cha}}+W_{\text{discha.T}}\tau_{\text{discha}}} \tag{20}$$

3.4 Calculation process

This work is carried out by using MATLAB. When calculating the thermodynamic parameters and thermal economy for the flexible operation system of CFPU, it should be assumed as follows:

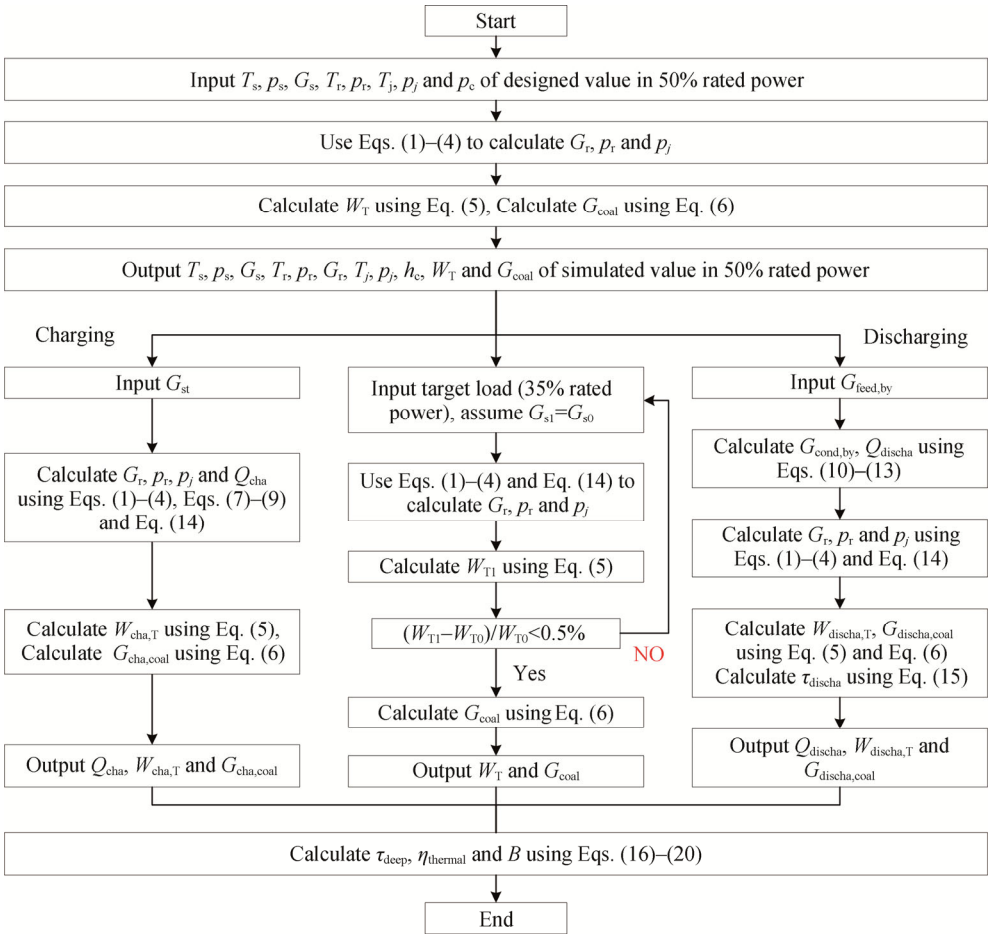

Fig. 3 Calculation flow chart of flexible operation

(1) The boiler must be operated at a stable combustion load; the boiler load can fluctuate in a small range, and the boiler is considered as a black box [26, 27].

(2) The pressure and temperature of main steam remain constant by adjusting the coal mass flow rate into the boiler during heat charging and discharging processes.

(3) The steam extraction temperature of RH1-RH7 should be constant under any working condition.

(4) The pressure loss of the extracted reheat steam is ignored.

(5) The pressurized water is saturated water in the pressurized water tank.

(6) The molten salts are an ideal thermal energy storage material. It is considered that the temperature of the molten salt in the "hot" and "cold" tank is almost constant, so its thermophysical property parameters (such as specific heat, density and thermal conductivity) are almost constant.

Fig. 3 shows the calculation process of the thermodynamic parameters for flexible operation system of CFPU. Firstly, the thermal parameters of 50% rated power will be given; the deviations between the simulation value and the design value are analyzed, and the power output of 35% rated power is calculated by using direct coal reduction method. Secondly, the power output of the CFPU is calculated by extracting the reheat steam in heat charging process. Thirdly, the power output of the CFPU is calculated by releasing the stored heat in heat discharging process. Finally, the deep peak shaving time, thermal efficiency and coal consumption rate are calculated.

4. Results and Discussion

4.1 Deviation analysis

According to the calculation flow chart shown in Fig. 3, the parameters of the traditional CFPU at 50% rated power are calculated. The deviations of main parameters between designed and simulation value are obtained. The deviation is defined as Eq. (21).

$$\text{Deviation} = \frac{\text{Designed value} - \text{Simulation value}}{\text{Designed value}} \times 100\% \quad (21)$$

The deviation analysis is shown in Table 4. The deviation of 4.65% in the extracted steam pressure of RH1 is the biggest. The work of steam is calculated by enthalpy, the influence of steam pressure on enthalpy is small, and this error can be ignored. Other deviations are less than that of the extracted steam pressure of RH1. The engineering accuracy requirements are satisfied [28]. So this novel model can be used to calculate the flexible operation of CFPU.

Table 4 Deviation analysis

	Designed value	Simulation value	Deviation/%
W_T/MW	300.11	300.03	0
p_s/kPa	9774	9774	0
G_s/t·h^{-1}	900.11	894.30	0.65
p_r/kPa	1750	1713	2.11
p_1/kPa	3094	2950	4.65
p_2/kPa	1944	1906	1.95
p_3/kPa	1059	1052	0.66
p_4/kPa	530	527	0.57
p_5/kPa	324	321	0.93
p_6/kPa	128	127	0.78
p_7/kPa	43	43	0

4.2 Impact of extracted reheat steam flow rate on power output and heat charging power

The influence of the extracted reheat steam flow rate on the power output and heat charging power is studied because they are utilized to calculate the deep peak shaving time, thermal efficiency and coal consumption rate for flexibility operation performance evaluation. Fig. 4 shows the impact of the extracted reheat steam flow rate on the power output and heat charging power in the heat charging process. The power output decreases from 300.03 MW to 210.07 MW when the steam extraction flow rate increases from 0 to 270.70 t·h^{-1}. The increase in the extracted reheat steam flow rate results in the decrease in the reheat steam flowing into IPT and LPT, so the power output of CFPU is decreased. The peak shaving capacity of 15% rated power can be reached when the power output is reduced from 300.03 MW to 210.07 MW. The power output of the unit with 200 kPa pressurized water is equal to that with 400 kPa pressurized water in the heat charging process due to the same parameters of the extracted steam. Meanwhile, the total heat charging power increases with the increase in the extracted reheat steam flow rate for the sensible and latent heat of steam is all stored in the molten salts and pressurized water. When the extracted reheat steam flow rate reaches 270.70 t·h^{-1}, the total heat charging power with 200 kPa or 400 kPa pressurized water all is 248.53 MW for the same parameters of the extracted reheat steam.

Although the pressure of pressurized water has no effect on power output and heat charging power during the heat charging process, the pressure of pressurized water affects the flow rate of pressurized water. Fig. 5 shows the impact of the extracted reheat steam flow rate on the flow rate of molten salts and pressurized water. It can be seen that with the increase in the extracted reheat steam flow rate, the molten salts flow rate and

pressurized water flow rate is increased. During this process, the molten salts flow rate is equal with 200 kPa or with 400 kPa pressurized water due to the same extracted steam parameters of SMHE, while the flow rate of 200 kPa pressurized water is higher than that of 400 kPa pressurized water because the higher pressure pressurized water has a bigger heat storage density. When the extracted reheat steam flow rate is 270.70 t·h^{-1}, the pressurized water flow rate of 200 kPa pressurized water is 2481.50 t·h^{-1}, which is higher than that of 400 kPa pressurized water.

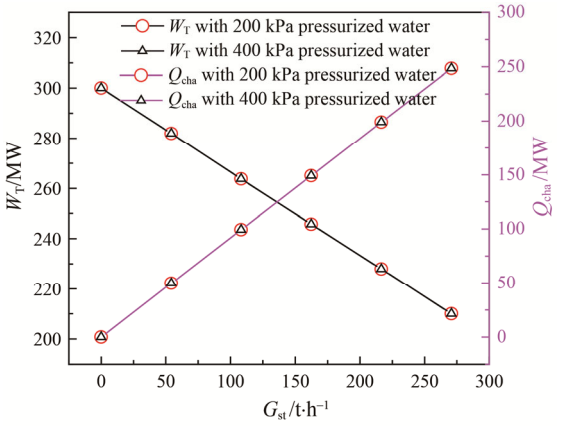

Fig. 4 Impact of extracted reheat steam flow rate on power output and heat charging power

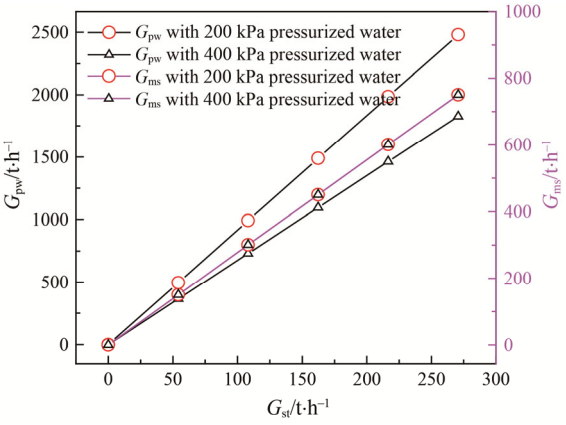

Fig. 5 Impact of extracted reheat steam flow rate on molten salts and pressurized water flow rate

4.3 Impact of pressurized water pressure on power output and coal mass flow rate

The main objective of the flexible operation of CFPU is to increase the deep peak shaving time as much as possible, so it is necessary to analyze the maximum heat discharging power at different heat discharging mode. The results show that when the condensate water is all replaced by the heated pressurized water from PWT; that is the condensate water flowing into RH5-RH7 is 0, the heat discharging power reaches the maximum, under which condition the bypassed condensate water flow rate of IPM-I, IPM-II, RFM-I and RFM-II is 753.59 t·h^{-1}, 792.88 t·h^{-1}, 717.31 t·h^{-1} and 734.72 t·h^{-1}, respectively. The maximum heat discharging power of IPM-I, IPM-II, RFM-I and RFM-II is 73.97 MW, 105.69 MW, 70.40 MW and 97.94 MW, respectively, by which the deep peak shaving time, thermal efficiency and coal consumption rate can be calculated in the later section. The impact of pressurized water pressure on power output and coal mass flow rate are investigated at the maximum heat discharging power, as shown in Table 5.

It can be seen that the pressurized water pressure makes contributions to the heat discharging power. The greater heat discharging power with the higher pressurized water pressure results in the greater flow rate of bypassed feed water, while the more extracted steam flow rate of RH1-RH3 can be replaced during heat discharging process. For example, the power output of IPM-I is 318.17 MW, while it is 328.31 MW for IPM-II, the power output increment of IPM-II is 10.14 MW greater than that of IPM-I because the reduced extracted steam flow rate of RH1-RH3 in IPM-II is higher than that in IPM-I. Compared with 50% rated power, the coal mass flow rate of RFM-I and RFM-II is all decreased, respectively. This reason is that there is no the extracted steam from the LPT, and the extracted steam of RH1-RH3 is decreased during the heat discharging process, so the power output of the steam turbine increases. At the condition of constant power output (300.03 MW), the main steam flow rate and the coal mass flow rate can be reduced. The decrease of the coal mass flow rate of RFM-II is 6.79 t·h^{-1}, which is greater

Table 5 Impact of pressurized water pressure on power output and coal mass flow rate

Operation mode	50% rated power	IPM-I	IPM-II	RFM-I	RFM-II
Bypassed condensate water flow rate/t·h^{-1}	0	753.59	792.88	717.31	734.72
Bypassed feed water flow rate/t·h^{-1}	0	165.85	238.45	160.40	226.50
Molten salts flow rate/t·h^{-1}	0	232.69	332.50	221.48	308.11
Heat discharging power/MW	0	73.97	105.69	70.40	97.94
Power output/MW	300.03	318.17	328.31	300.16	300.04
Main steam flow rate/t·h^{-1}	894.30	894.30	894.30	845.80	820.60
Coal mass flow rate/t·h^{-1}	94.79	95.09	95.23	90.35	88

than that of RFM-I, for the reason that the heat discharging power of RFM-II is bigger than that of RFM-I. In addition, the heat discharging power of IPM-I is greater than that of RFM-I because the main steam flow rate of RFM-I is lower than that of IPM-I. The same reason is that the heat discharging power of IPM-II is greater than that of RFM-II.

4.4 Impact of heat charging power on deep peak shaving time

The deep peak shaving time of CFPU is a key factor to evaluate the peak shaving capacity of the unit. The deep peak shaving time is calculated according to Eq. (15) and Eq. (16) by taking the heat discharging power in Table 5 and the heat charging power in Fig. 4. Fig. 6 shows the impact of the heat charging power on the deep peak shaving time. The raising heat charging power results in the decreasing of the deep peak shaving time. The reason is that the greater the heat storage capacity is, the more heat discharging time is required when the heat discharging power is constant, which results in the shorter time of deep peak shaving that can be participated in every day. The deep peak shaving time of the four operation modes is RFM-I, IPM-I, RFM-II and IPM-II from small to large. This is because the greater the heat discharging power results in the shorter the heat discharging time when the heat charging power is same. When the unit achieves the deep peak shaving of increasing by 15% rated power with IPM-I, IPM-II, RFM-I and RFM-II, the deep peak shaving time is 5.90 $h \cdot d^{-1}$, 7.63 $h \cdot d^{-1}$, 5.69 $h \cdot d^{-1}$ and 7.24 $h \cdot d^{-1}$, respectively. So the IPM has the advantages of higher deep peak shaving time than that of RFM for flexible operation.

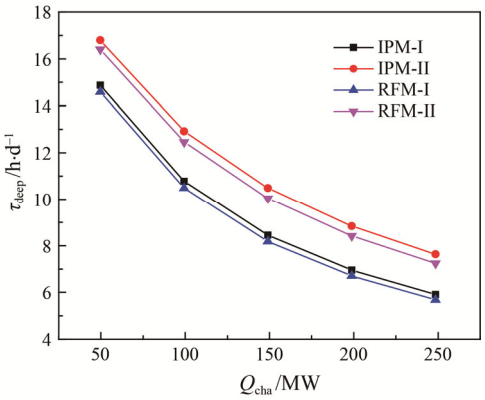

Fig. 6 Impact of heat charging power on deep peak shaving time

4.5 Impact of heat charging power on thermal efficiency and coal consumption rate

When calculating the thermal efficiency and coal consumption rate of the CFPU in a whole heat charging and heat discharging cycle, the data described in Section 4.4 is selected as the calculation data.

Fig. 7 shows the impact of the heat charging power on the thermal efficiency of CFPU in different heat discharging mode. The thermal efficiency is decreased with the increasing of the heat charging power because the steam flowing into the IPT and LPT decreases, and its pressure reduced, so the power output of the IPT and LPT driven by enthalpy drop of steam is decreased and the heat rate of CFPU is increased, which results in the reduction of the thermal efficiency.

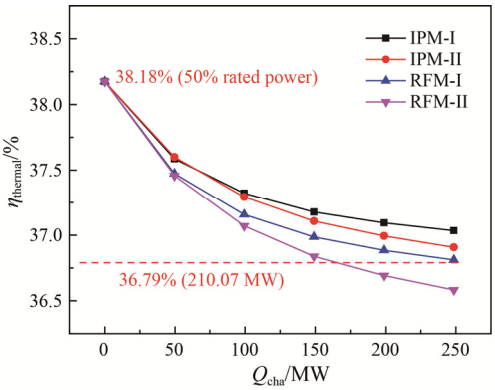

Fig. 7 Impact of heat charging power on thermal efficiency

Because the stored heat is released to heat the bypassed feed water and replace the condensate water, the additional heat rate entering into CFPU increases. The greater the heat discharging power results in the more additional heat rate, which is the reason why the thermal efficiency of IPM-I is larger than that of IPM-II at the same charging power. The steam pressure at each stages of the turbine decreases when the unit reduces the main steam flow rate to keep the unit power output constant, which results in the reduction of the thermal efficiency. Because the main steam flow rate of RFM-I is larger than that of RFM-II, the thermal efficiency of RFM-I is larger than that of RFM-II. They are the reasons why the thermal efficiency of IPM-I is larger than that of RFM-I and the thermal efficiency of IPM-II is larger than that of RFM-II.

When the CFPU completes the deep peak shaving by taking the working condition of the increase of 15% rated power and the maximum heat discharging power, the thermal efficiency of IPM-I, IPM-II, RFM-I and RFM-II is 37.04%, 36.91%, 36.81% and 36.58%, respectively. Where, the thermal efficiency of IPM-I, IPM-II, RFM-I and RFM-II is lower than that of 50% rated power; the thermal efficiency of IPM-I, IPM-II and RFM-I is greater than that of 35% rated power (210.07 MW) without utilizing the steam extraction, and the thermal efficiency of RFM-II is lower than that of 35% rated power (210.07 MW) without utilizing the steam extraction. So the IPM has more advantages than the RFM from the perspective

of the thermal efficiency.

Fig. 8 shows the impact of heat charging power on the coal consumption rate of the CFPU. From Eqs. (17)–(20), it is found that the lower thermal efficiency of the CFPU will inevitably result in the higher coal consumption rate. The coal consumption rate is increased with the raising of the heat charging power because the thermal efficiency decreases with the increasing of the heat charging power as described in Fig. 7. The coal consumption rate of IPM-I is smaller than that of IPM-II because the thermal efficiency of IPM-I is larger than that of IPM-II. The same reason is that the coal consumption rate of RFM-I is smaller than that of RFM-II. At the same time, the coal consumption rate of IPM-I is smaller than that of RFM-I because the thermal efficiency of IPM-I is larger than that of RFM-I, and the coal consumption rate of IPM-II is smaller than that of RFM-II because the thermal efficiency of IPM-II is larger than that of RFM-II.

When the CFPU completes the deep peak shaving by taking the working condition of the increase of 15% rated power and the maximum heat discharging power, the coal consumption rate of IPM-I, IPM-II, RFM-I and RFM-II is 325.45 $g\cdot kW^{-1}\cdot h^{-1}$, 326.54 $g\cdot kW^{-1}\cdot h^{-1}$, 327.40 $g\cdot kW^{-1}\cdot h^{-1}$ and 329.42 $g\cdot kW^{-1}\cdot h^{-1}$, respectively. The coal consumption rate of IPM-I, IPM-II, RFM-I and RFM-II is larger than that of 50% rated power, and the coal consumption rate of IPM-I, IPM-II and RFM-I is lower than that of 35% rated power (210.07 MW) without utilizing the steam extraction, and the coal consumption rate of RFM-II is higher than that of 35% rated power (210.07 MW) without utilizing the steam extraction. The IPM has more advantages than the RFM in terms of the coal consumption rate.

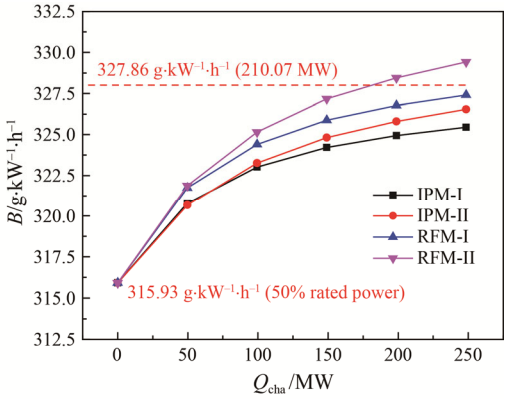

Fig. 8 Impact of heat charging power on coal consumption rate

5. Conclusions

In order to increase large scale renewable energy access to the grid, the deep peak shaving of the coal-fired power unit needs to be achieved. This paper proposes a new flexible operation system to achieve the deep peak shaving by integrating with reheat steam extraction and heat storage. The load of coal-fired power unit can be further reduced at a stable load. The following conclusions are drawn:

(1) The out power can be further reduced from 300.03 MW to 210.07 MW by reheat steam extraction with the flow rate of 270.70 $t\cdot h^{-1}$, which increases the deep peak shaving capacity by 15% rated power.

(2) The increasing power output mode operates during the peak period of power consumption; increasing the pressure of pressurized water can increase the power output of the unit. The deep peak shaving time and the thermal efficiency are 7.63 $h\cdot d^{-1}$ and 36.91%, respectively.

(3) The reducing fuel mode operates during the peak period of power consumption at a constant power, increasing the pressure of pressurized water can reduce the coal mass flow rate into the boiler. The deep peak shaving time and the thermal efficiency are 7.24 $h\cdot d^{-1}$ and 36.58%, respectively.

(4) The increasing power output mode has the advantages of higher deep peak shaving time and thermal efficiency than that of the reducing fuel mode. If necessary, the increasing power output mode is recommended as the preferred scheme for the flexible operation of the coal-fired power unit.

Acknowledgements

This work was supported by the National Natural Science Foundation of China (Grant No. 52076006), and the Inner Mongolia Science and Technology Major Project (Grant No. 2021ZD0036).

References

[1] Yuan Y., Cai F., Yang L., Renewable energy investment under carbon emission regulations. Sustainability, 2020, 12: 1–15.

[2] Zhang H., Liang W., Liu J., et al., Modeling and energy efficiency analysis of thermal power plant with high temperature thermal energy storage (HTTES). Journal of Thermal Science, 2020, 29(4): 1025–1035.

[3] Zhang M., Yang Z., Liu L., et al., Impact of renewable energy investment on carbon emissions in China - An empirical study using a nonparametric additive regression model. Science of the Total Environment, 2021, 785: 1–11.

[4] Wang Y., Lou S., Wu Y., et al., Flexible operation of retrofitted coal-fired power plants to reduce wind curtailment considering thermal energy storage. IEEE

Transactions on Power Systems, 2020, 35(2): 1178–1187.
[5] Wang Y., Lou S., Wu Y., et al., Coordinated planning of transmission expansion and coal-fired power units flexibility retrofits to accommodate the high penetration of wind power. IET Generation Transmission & Distribution, 2019, 13(20): 4702–4711.
[6] Ioannis A., Dimitrios R., Sotirios K., et al., Review of process modeling of solid-fuel thermal power plants for flexible and off-design operation. Energies, 2020, 13(24): 1–41.
[7] Zhou Y., Wang D., An improved coordinated control technology for coal-fired boiler-turbine plant based on flexible steam extraction system. Applied Thermal Engineering, 2017, 125: 1047–1060.
[8] Wang C., Zhao Y., Liu M., et al., Peak shaving operational optimization of supercritical coal-fired power units by revising control strategy for water-fuel ratio. Applied Energy, 2018, 216: 212–223.
[9] Zhang K., Zhao Y., Liu M., et al., Flexibility enhancement versus thermal efficiency of coal-fired power units during the condensate throttling processes. Energy, 2021, 218: 1–14.
[10] Wang W., Liu J., Zeng D., et al., Flexible electric power control for coal-fired units by incorporating feedwater bypass. IEEE Access, 2019, 7: 91225–91233.
[11] Zhao Y., Wang C., Liu M., et al., Improving operational flexibility by regulating extraction steam of high pressure heaters on a 660 MW supercritical coal-fired power unit: A dynamic simulation. Applied Energy, 2018, 212: 1295–1309.
[12] Wang W., Jing S.G., Sun Y., et al., Combined heat and power control considering thermal inertia of district heating network for flexible electric power regulation. Energy, 2019, 169: 988–999.
[13] Yoshiba F., Hanai Y., Watanabe I., et al., Methodology to evaluate contribution of thermal power plant flexibility to power system stability when increasing share of renewable energies: Classification and additional fuel cost of flexible operation. Fuel, 2021, 292: 1–10.
[14] Wang C., Song J., Zhu L., et al., Peak shaving and heat supply flexibility of thermal power plants. Applied Thermal Engineering, 2021, 193: 1–8.
[15] Richter M., Oeljeklaus G., Görner K., Improving the load flexibility of coal-fired power units by the integration of a thermal energy storage. Applied Energy, 2019, 236: 607–621.
[16] Trojan M., Taler D., Dzierwa P., et al., The use of pressure hot water storage tanks to improve the energy flexibility of the steam power unit. Energy, 2019, 173: 926–936.
[17] Li D., Wang J., Study of supercritical power plant integration with high temperature thermal energy storage for flexible operation. Journal of Energy Storage, 2018, 20: 140–152.
[18] Krüger M., Muslubas S., Loeper T., et al., Potentials of thermal energy storage integrated into steam power plants. Energies, 2020, 13(9): 1–13.
[19] Sun Y., Xu C., Xin T., et al., A comprehensive analysis of a thermal energy storage concept based on low-rank coal pre-drying for reducing the minimum load of coal-fired power plants. Applied Thermal Engineering, 2019, 156: 77–90.
[20] Gu Y., Xu J., Chen D., et al., Overall review of peak shaving for coal-fired power units in China. Renewable and Sustainable Energy Reviews, 2016, 54: 723–731.
[21] Wei H., Lu Y., Yang Y., et al., Research on influence of steam extraction parameters and operation load on operational flexibility of coal-fired power plant. Applied Thermal Engineering, 2021, 195: 1–10.
[22] Wu Y., Li Y., Lu Y., et al., Novel low melting point binary nitrates for thermal energy storage applications. Solar Energy Materials & Solar Cells, 2017, 164: 114–121.
[23] Verda V., Colella F., Primary energy savings through thermal storage in district heating networks. Energy, 2011, 36: 4278–4286.
[24] Wu J., Hou H., Hu E., et al., Performance improvement of coal-fired power generation system integrating solar to preheat feed water and reheated steam. Solar Energy, 2018, 163: 461–470.
[25] Zhai R., Liu H., Li C., et al., Analysis of a solar-aided coal-fired power generation system based on thermo-economic structural theory. Energy, 2016, 102: 375–387.
[26] Wu J., Hou H., Yang Y., The optimization of integration modes in solar aided power generation (SAPG) system. Energy Conversion and Management, 2016, 126: 774–789.
[27] Zhang N., Hou H., Yu G., et al., Simulated performance analysis of a solar aided power generation plant in fuel saving operation mode. Energy, 2019, 166: 918–928.
[28] Liu H., Zhai R., Patchigolla K., et al., Off-design thermodynamic performances of a combined solar tower and parabolic trough aided coal-fired power unit. Applied Thermal Engineering, 2021, 183: 1–15.